

## NONDESTRUCTIVE LASER CONFOCAL SCANNING MICROSCOPY AND SYNCHROTRON MICROTOMOGRAPHY OF SINGLE STARDUST AND ANALOG TRACKS IN AEROGEL

**KEYSTONES.** D. S. Ebel<sup>1</sup>, J. L. Mey<sup>1</sup>, and M. L. Rivers<sup>2</sup>. <sup>1</sup>American Museum of Natural History, Central Park West at 79<sup>th</sup> Street, New York, NY 10024 ([debel@amnh.org](mailto:debel@amnh.org); [mey@amnh.org](mailto:mey@amnh.org)), <sup>2</sup>Department of the Geophysical Sciences, University of Chicago, 5640 South Ellis Ave., Chicago, IL 60637 ([rivers@cars.uchicago.edu](mailto:rivers@cars.uchicago.edu)).

**Introduction:** Particles of Comet Wild 2 collected in silica aerogel tiles at ~6 km/sec by the Stardust mission are distributed as ‘keystones’. These are thin (<1mm) triangular sections containing whole or partial impact tracks [1,2]. Small grains, embedded in melted silica, are distributed along a track as the comet particle fragments on impact [3]. Our goal has been to collect maximum information on grain location, composition and size, and the original relationship between grain fragments. We use non- or minimally-destructive techniques, prior to flattening, sectioning, or other processing that destroys information. We have demonstrated synchrotron x-ray computer-assisted microtomography (XR-CMT) ‘lambda’ tomography on analog aerogel tiles shot with Allende dust, as a tool to serially image whole tiles [4,5]. Here, we report on XR-CMT of a stardust keystone containing a whole ~1mm long track at 1.03  $\mu\text{m}/\text{voxel}$  edge. We also report on application of both reflected and transmitted laser scanning confocal microscopy (LSCM) to an analog keystone containing tracks shot with basalt. We compare these two 3D imaging techniques with images obtained using a research optical microscope (OM). By March 2007, we will have confocal images of the stardust track, and complementary tomographic data on the analog track.

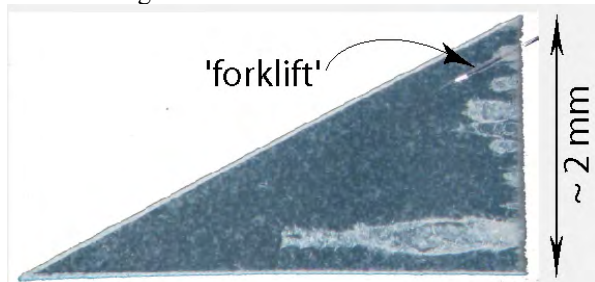


Fig. 1: Entire keystone, analog basalt-shot aerogel.

**Samples:** Stardust track #82 (C2092,1,82,00) was imaged in full during the preliminary examination period [6]. In comprehensive testing of analog samples, powdered, unseived (1-100  $\mu\text{m}$ ) USGS Fe-basalt glass standard NKT-1G [7] was shot (5-Dec-06, by Mark Burchell at the U. Kent gas gun) into uniform  $\rho = 25 \text{ kg/m}^3$  aerogel (average  $\rho$  of density-graded flight aerogel) at 5.88 km/sec [8,9]. A keystone of this analog shot was provided by C. Snead (U. C. Berkeley).

**Technique:** XR-CMT was done at the Consortium for Advanced Radiation Sources beamline 13BM, Ad-

vanced Photon Source, Argonne National Lab, at 12KeV [10], at 1.03  $\mu\text{m}/\text{pixel}$  edge (1.34 x 1.06 mm field of view) spatial resolution (unbinned data). Exposure times, data binning, and phase contrast were explored, to optimize resolution and grain contrast.

LSCM was done at the AMNH Microscopy and Imaging Facility, using the Zeiss Axiovert 100 equipped with 3 lasers (458 nm Ar, 543 and 643 HeNe). Images acquired with the 458 nm (Ar) laser for optimal resolution were post-processed using LSM-510 software, and Imaris (Bitplane AG). Pixel resolution  $r$  is determined by optical objective and binning in the detector. Raw data are a stack of  $n$  optical slices,  $2048 \times 2048 \times d$  ( $d$  is the thickness of the planar volume of laser excitation), at a series of depths (focal lengths along  $z$ ) in the sample. Each datum is an 8-bit light intensity value (256 grayscales). To reduce data size, we declined to use the 12-bit collection option). Each slice records light reflected or transmitted from a planar volume in the sample of thickness  $d$ . Each pixel records light intensity from a volume  $r * r * d$ . Sequential frames are set to overlap  $\frac{1}{2}$  thickness because accuracy of focus is highest in the center of each optical slice.

Raw data reprocessed in Imaris yields a 3D data volume from which 2D (flat) images or screenshots can be extracted by either (1) orthogonal projection, which preserves scale, or (2) perspective projection, in which scaling varies slightly depending on depth in the sample and viewing angle (e.g., Fig. 2,3).

The resolution of the scan of the terminal particle region is better than the resolution of the optics in our microscope, specified by the vendor at 0.3  $\mu\text{m}$ , and also has superior depth resolution in the processed images, compared to a standard optical microscope. The processed data allows quantification of 3D spatial relationships between particles in the tracks, up to 3 mm along the light path ( $z$ ). LSCM and tomography data sets larger than 1 GB were processed on 64-bit PC (XP64 OS) and SGI Origin 2000 boxes, respectively. A large variety of static and dynamic 2D and 3D image products can be produced from these data sets.

**Results:** XR-CMT data for track C2092 are shown in Fig. 4 (cf. [6]), a sequence of each fifth parallel slice in a cropped tomography volume. In rotating the sample, the field of view includes the relatively high-

density glass forklift, causing artifacts where the forklift and track are present in the same horizontal plane. Table 1: Summary of LSCM scans (each 0.4 – 1.2 GB raw data): track portion, objective, optical slice thickness ( $d$ ,  $\mu\text{m}$ ), sec/frame ( $t$ ), pixel resolution ( $r$ ,  $\mu\text{m}/\text{pxl}$ ).

	Subject	Obj	$n$	$d$	$t$	$r$
1	Entire	5x	200	5.11	15	1.123
2	Partial	10x	100	3.43	60	0.610
3	Terminal	20x	100	1.75	60	0.134

LSCM data was initially reconstructed as volume-rendered point-clouds (e.g., Fig. 2). No spherical aberration was observed, however, marked axial distortion (grain image elongation  $\parallel z$ ) may be an artifact of refraction at the air/aerogel interface. Usually, LSCM is done with a drop of oil, of similar refractive index as the sample, to minimize the bending of light along the laser path. Alternatively, light may be bouncing between the parallel surfaces of the keystone. Future work includes an effort to correct this axial distortion by modifying optics or post-processing.

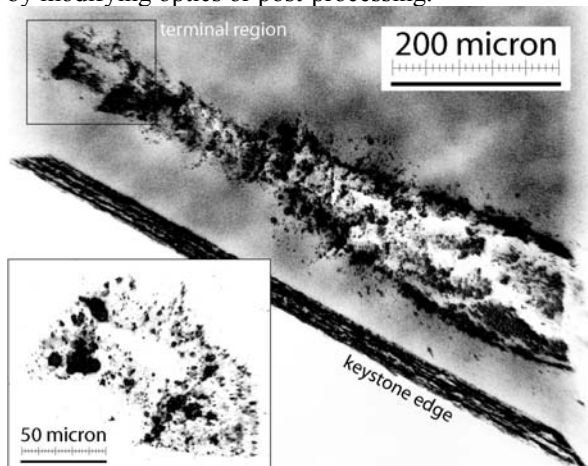


Fig. 2: LSCM perspective projection (10x) of most of large track. Scale is estimated(see text).

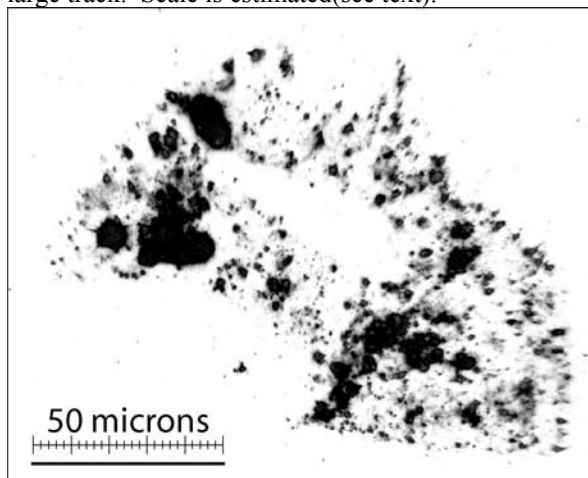


Fig. 3: LSCM perspective projection (20x) of terminal particle region. Scale is estimated (see text).

**Conclusions:** LSCM is highly successful for straightforward 3D characterization of embedded grain geometries in whole stardust tracks at high spatial resolution. LSCM is a direct imaging technique, supplemented by post-imaging interpolation. XRCMT requires reconstruction of x-ray attenuation by volume elements, introducing noise. However, recent developments in XRCMT allow nm-scale study of individual grains, which LSCM cannot approach [11,12]. The preliminary work described above shows that the aerogel in keystones serves as a transparent medium with miniscule laser interaction artifacts. Processed confocal data allows direct quantification of 3D spatial relationships between particle fragments in the keystone tracks, in all 3 dimensions. LSCM is a standard bench-top tool allowing depth resolution far superior to any other optical system. We should be able to distinguish minerals from each other in LSCM by their optical properties.

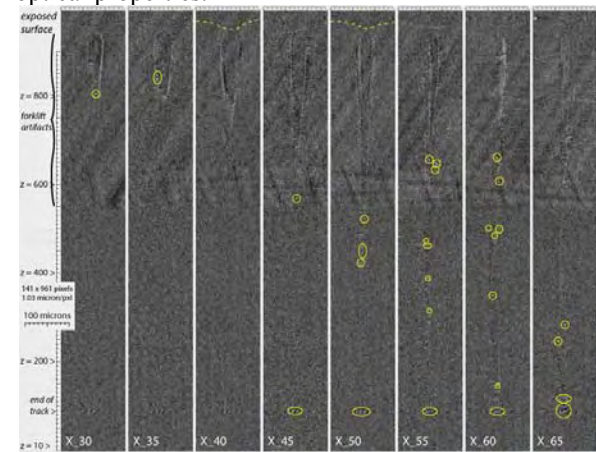


Fig. 4: XRCMT sequence, 1.03  $\mu\text{m}/\text{pixel}$ . Grains are circled. Dashed lines indicate inferred location of entry hole in aerogel top.

**References:** [1] Burchell M.J. *et al.* (2006) *Ann. Rev. Earth Planet. Sci.* 34: 385-418. [2] Westphal A.J. *et al.* (2004) *Meteor. Planet. Sci.*, 39, 1375-1386. [3] Brownlee *et al.* (2006) *Science* 314: 1711-1716. [4] Ebel D.S. & Rivers M.L. (2005) *Meteor. & Planet. Sci. Suppl.*, 32, A42 (#5299) [5] Ebel D.S. & Rivers M.L. (2006) August mtg. of SPIE. [6] <http://research.amnh.org/users/debel/tomo-aps/aerogel1.html> [7] Potts P.J. *et al.* (2006) *Geostands. & Geoanal. Res.* 30. [8] Burchell M.J. *et al.* (2007) *Meteor. & Planet. Sci.* (submitted). [9] Kearsley *et al.* 2006 astro.ph.12013K [10] Ebel D.S. *et al.* (2007) *Meteor. & Planet. Sci.* (in press). [11] Uesugi K. *et al.* (2001) *Proc. SPIE* 4503: 291. ([http://www.spring8.or.jp/pdf/en/res\\_fro/01-02/114-115.pdf](http://www.spring8.or.jp/pdf/en/res_fro/01-02/114-115.pdf)). [12] Attwood D. (2006) *Nature* 442: 642-643. This research was funded by NASA through NNG06GE42G (DSE). Use of the APS was supported by the U.S. Department of Energy, Office of Science, Office of Basic Energy Sciences, under Contract No. DE-AC02-06CH11357.